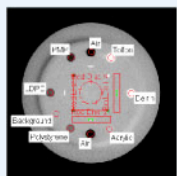


DIAGNOSTIC IMAGING QC SOLUTIONS

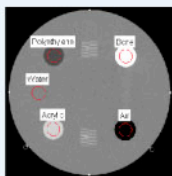
FROM RADIOLOGICAL IMAGING TECHNOLOGY, INC.

Radia Diagnostic performs automated phantom analysis in seconds. The simple, easy-to-use software tools provide complete scoring of all phantom parameters with precision and accuracy. All modules come equipped with tracking, trending and hands-free automation features designed to streamline your imaging QC workflow.

SPECIFIC MODULES & PHANTOMS

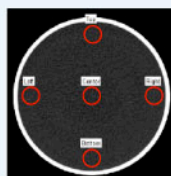


CATPHAN®
500/600 Series



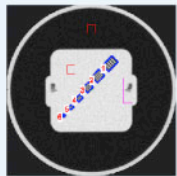
ACR CT
(Gammex 464)

CT/CBCT: Radia Diagnostic features the most robust and automated CT/CBCT phantom analysis on the market. Easily score vendor-supplied and ACR test phantoms with fast, quantitative, repeatable results for HU accuracy and constancy, geometric distortion, slice thickness, contrast/noise, and resolution. Analyze dental CBCT images with results for uniformity/noise, geometric distortion, high-density artifacts, low contrast detectability, and resolution.

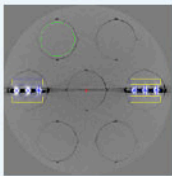


Universal CT Water Phantom:

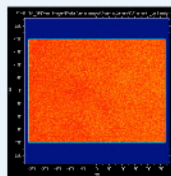
This uniformity test allows you to easily adjust the size and position of the analysis area to match any CT water phantom. This routine is perfect for daily axial and helical uniformity measurements.



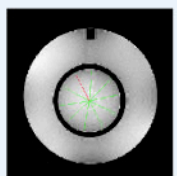
GE CT



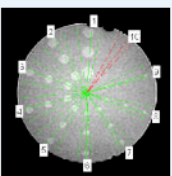
Leeds Sedentex
Dental CBCT



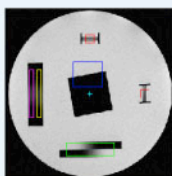
Gamma Camera: Easily measure the Intrinsic Flood Field Uniformity (NEMA NU 1-2012) parameters and perform automated analysis of integral uniformity, differential uniformity, and defective pixels for modern, rectangular gamma cameras.



ACR MRI



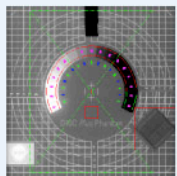
ACR Small MRI



Leeds MagIQ

MRI: ACR MRI and ACR Small MRI (Extremity and Breast) phantom results are easily quantified, tracked, and reported, providing you with robust measurements for resolution, slice thickness, geometric accuracy, uniformity/noise/signal ghosting, and low contrast detectability.

Analyze Leeds MagIQ images with results for contrast, geometric distortion, resolution, slice thickness, and uniformity/noise.



DR/CR kV: Perform all phantom parameters including contrast stepwedge, geometric accuracy, low contrast detection, MTF, noise, and uniformity. Supported phantoms include IBA Primus® L (including couch placement analysis), Leeds TOR-18 FG, PTW NORMI®-4 FLU, and DISC Plus.



ACR FFDM: Perform complete scoring of this phantom to full requirements. Scores fibers, specs and masses to half a point. Score contrast to noise, signal to noise, and insert size.

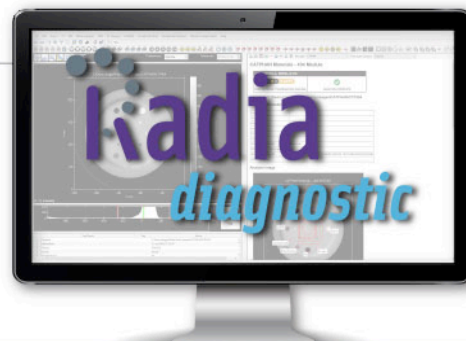
AUTOMATION & CUSTOMIZATION FEATURES

Complete Automation: Use Cerberus to perform hands-free, automated phantom analysis. Cerberus automatically monitors folders, pin-points files, and analyzes them in the background of your machine.

Tracking & Trending: RITtrend™ is the all-in-one statistical database solution for all of your department's measurements. Export full reports of all imaging tests with a single click and trend results over time.

RITtrend™ is a trademark of Radiological Imaging Technology, Inc.

Tolerance Customization: RIT's Tolerance Manager sets tolerance values and pass/fail criteria for every measurement, and preference profiles can be precisely tailored to each individual machine in use.



CLICK TO SCHEDULE A VIRTUAL SOFTWARE DEMO TODAY!



RADIMAGE.COM

+1.719.590.1077 // sales@radimage.com // Connect with us on social media @RIT4QA  

© 2021, Radiological Imaging Technology, Inc.

CATPHAN® is a registered trademark of The Phantom Laboratory. NORMI® is a registered trademark of PTW. Primus® is a registered trademark of IBA.

Determinants of the reliability of ultrasound tomography sound speed estimates as a surrogate for volumetric breast density

Zeina G. Khodr

Department of Health and Human Services, Division of Cancer Epidemiology and Genetics, National Cancer Institute, 9609 Medical Center Drive MSC 9774, Bethesda, Maryland 20892

Mark A. Sak

Karmanos Cancer Institute, Wayne State University, 4100 John R, Detroit, Michigan 48201

Ruth M. Pfeiffer

Department of Health and Human Services, Division of Cancer Epidemiology and Genetics, National Cancer Institute, 9609 Medical Center Drive MSC 9774, Bethesda, Maryland 20892

Nebojsa Duric and Peter Littrup

Karmanos Cancer Institute, Wayne State University, 4100 John R, Detroit, Michigan 48201 and Delphinus Medical Technologies, 46701 Commerce Center Drive, Plymouth, Michigan 48170

Lisa Bey-Knight

Karmanos Cancer Institute, Wayne State University, 4100 John R, Detroit, Michigan 48201

Haythem Ali and Patricia Vallieres

Henry Ford Health System, 2799 W Grand Boulevard, Detroit, Michigan 48202

Mark E. Sherman

Division of Cancer Prevention, National Cancer Institute, Department of Health and Human Services, 9609 Medical Center Drive MSC 9774, Bethesda, Maryland 20892

Gretchen L. Gierach^{a)}

Department of Health and Human Services, Division of Cancer Epidemiology and Genetics, National Cancer Institute, 9609 Medical Center Drive MSC 9774, Bethesda, Maryland 20892

(Received 21 November 2014; revised 19 August 2015; accepted for publication 21 August 2015; published 8 September 2015)

Purpose: High breast density, as measured by mammography, is associated with increased breast cancer risk, but standard methods of assessment have limitations including 2D representation of breast tissue, distortion due to breast compression, and use of ionizing radiation. Ultrasound tomography (UST) is a novel imaging method that averts these limitations and uses sound speed measures rather than x-ray imaging to estimate breast density. The authors evaluated the reproducibility of measures of speed of sound and changes in this parameter using UST.

Methods: One experienced and five newly trained raters measured sound speed in serial UST scans for 22 women (two scans per person) to assess inter-rater reliability. Intrarater reliability was assessed for four raters. A random effects model was used to calculate the percent variation in sound speed and change in sound speed attributable to subject, scan, rater, and repeat reads. The authors estimated the intraclass correlation coefficients (ICCs) for these measures based on data from the authors' experienced rater.

Results: Median (range) time between baseline and follow-up UST scans was five (1–13) months. Contributions of factors to sound speed variance were differences between subjects (86.0%), baseline versus follow-up scans (7.5%), inter-rater evaluations (1.1%), and intrarater reproducibility (~0%). When evaluating change in sound speed between scans, 2.7% and ~0% of variation were attributed to inter- and intrarater variation, respectively. For the experienced rater's repeat reads, agreement for sound speed was excellent (ICC = 93.4%) and for change in sound speed substantial (ICC = 70.4%), indicating very good reproducibility of these measures.

Conclusions: UST provided highly reproducible sound speed measurements, which reflect breast density, suggesting that UST has utility in sensitively assessing change in density. © 2015 American Association of Physicists in Medicine. [<http://dx.doi.org/10.1118/1.4929985>]

Key words: breast density, ultrasound tomography, reliability, reproducibility, change in breast density, breast cancer

1. INTRODUCTION

Increased percent mammographic breast density is a strong independent risk factor for breast cancer.¹ Mammography uses x-ray technology to create a 2D image of the compressed breast. The interaction between x-ray and breast tissue is used to calculate an indirect measure of breast density. Breast density is typically computed from the mammographic image by dividing the radio-opaque area, corresponding to epithelial and stromal tissues, by the total breast area, which includes both dense and nondense areas, the latter reflecting adipose tissue.^{2,3}

Over the past decade, calculations of breast density from mammographic images have evolved from qualitative measures [e.g., Wolfe's classification² and breast imaging reporting and data system (BI-RADS)⁴] to more objective measurements (e.g., visual assessment of percent breast density and computer-assisted thresholding methods).^{1,5} Although methods for measuring volumetric breast density from mammography have been developed,^{6,7} the 2D nature of mammographic images may represent an inherent limitation of this imaging technique.⁸ In addition, variability in protocols for mammogram acquisition, including machine settings, digital or film technique, degree of breast compression, and other factors may diminish reproducibility of density measures. Particularly, comparing serial images within one woman over time is difficult, as women are unlikely to be imaged repeatedly with the same mammography machine under identical conditions.⁹ Further, mammograms expose women to potentially harmful ionizing radiation, which limits the frequency with which examinations can be repeated and pose concerns about imaging young women who may be particularly susceptible.¹⁰ Magnetic resonance imaging (MRI) is an alternative method for measuring breast density, which uses a magnetic field and radio wave energy to provide a 3D image of organs without exposure to ionizing radiation.^{5,11–13} However, MRI is more expensive than mammography, not easily accessible, and requires special facilities in addition to intensive training.

Ultrasound tomography (UST), a novel imaging tool that uses sound speed measures, provides the ability to assess volumetric breast density of the uncompressed breast, similar to MRI, without many of the limitations of mammography.^{3,14} Sound speed has been shown to be a surrogate to mammographic measures of breast density, with statistically significant correlations with both BI-RADS density categories and computer-assisted quantitative measures of mammographic breast density.^{3,15–21} Of additional importance, UST provides the opportunity to conduct serial breast scans without the risk of ionizing radiation and to monitor changes in breast density over time.¹⁸ Obtaining reliable estimates of density change is clinically relevant as a growing number of studies have demonstrated that changes in breast density are associated with response to some breast cancer treatments, such as tamoxifen.^{22–26}

Previous studies have illustrated the technical aspects of volumetric breast density evaluation from UST sound speed images.^{3,15,27} Here, we aimed to assess the rater reliability

of UST sound speed estimates as a surrogate for volumetric breast density, using a prototype scanner,¹⁴ among a subset of participants enrolled in an ongoing study monitoring breast density changes over the course of a year. Demonstrating the reproducibility of sound speed measurements in the context of this study is critical, given that detecting changes in density over brief intervals requires excellent precision.

2. MATERIALS AND METHODS

2.A. Study population

The study population included a subset of women, with at least two UST serial breast scans available, enrolled between 2011 and 2012 in the Ultrasound Study of Tamoxifen.¹⁸ Briefly, participants 30–70 yr of age at baseline were recruited from the Barbara Ann Karmanos Cancer Institute (KCI) and Henry Ford Hospital (HFH) in Detroit, MI. Exclusion criteria included weight >250 lbs and breast diameter >20 cm (maximal allowable for scanner), pregnancy, breastfeeding, current breast implants, and active breast skin infections. Women underwent UST scans at baseline and had a second follow-up scan ranging from one month to 13 months after baseline. The contralateral breast was scanned in participants with a diagnosis of incident unilateral atypical lobular or ductal hyperplasia (ALH/ADH), ductal or lobular carcinoma *in situ* (DCIS/LCIS), or invasive breast cancer. The breast to be scanned was randomly selected in women without a diagnosis of ALH/ADH, DCIS/LCIS, or invasive breast cancer. During follow-up, study participants who developed an active breast skin infection, who had an excisional biopsy, or who had a mastectomy of the same breast scanned at baseline were excluded. The analytic population was comprised of 22 study participants who provided written informed consent. The study was approved by ethical boards at all participating institutions.

2.B. Ultrasound tomography

Participants were scanned with the Computed Ultrasound Risk Evaluation (CURE) UST prototype.¹⁴ Briefly, UST scans were performed while a patient was in the prone position with the breast to be scanned suspended in a water bath (Fig. 1). Breasts were scanned with a 20 cm ring-shaped transducer, consisting of 256 elements that transmit and receive ultrasound pulses, which was mounted on an automated gantry that progressively captured 40–100 coronal image slices beginning at the chest wall and progressing to the nipple. Unlike conventional ultrasound, UST provides four tomographic images: high-resolution reflection, low-resolution reflection, attenuation, and sound speed images. The present analysis focused on volumetric breast density as estimated through sound speed images.

Sound speed images were processed prior to analysis using the public domain software package ImageJ.²⁸ To begin, the first and last image slices, comprising boundaries of the breast tissue, were identified to remove images of the chest wall, pectoralis muscle, and the water bath (i.e., extending beyond

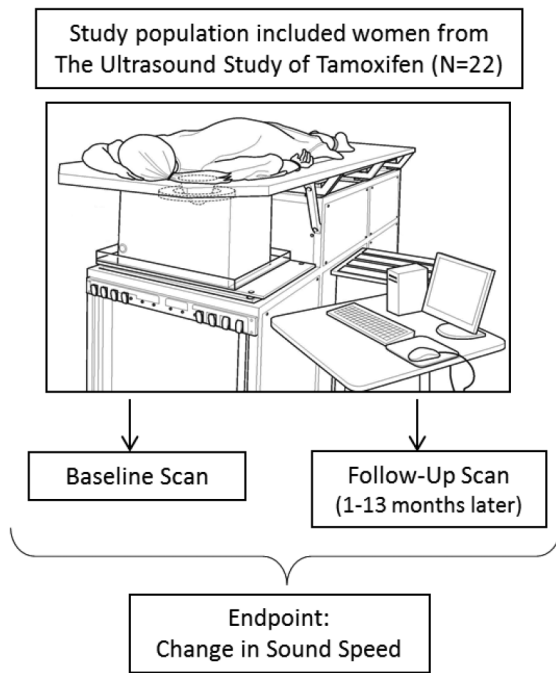


FIG. 1. Study design and depiction of the ultrasound tomography scanner, adapted from Duric *et al.* (Ref. 17).

the nipple; Fig. 2). A semiautomated method was used to differentiate the breast from the water bath as an ellipse, for each image slice, as thresholding techniques were not an option since the sound speed of the water bath falls within the expected range of the sound speed for breast tissue [Fig. 3(A)]. Next, dark ring artifacts, which were caused by slow moving surface waves when the transducer was closer to the breast (i.e., closer to the chest wall in larger breasts and specifically affecting breast tissue nearer to the skin surface)

and can decrease the overall measured sound speed, were eliminated [Fig. 3(B)]. Manual removal of dark ring artifact was done in ImageJ. A large ellipse was fit to encompass the breast tissue area, allowing the pixels related to the dark ring artifact, outside of the ellipse, to be cleared and set to zero. These artifacts were seen in approximately half of images. The median percentage of voxels removed was 7%, ranging from 0.4% to 28%. To analyze change in sound speed between serial scans, image files were restricted to a common volume that was contained within both scans. For tomograms included in the common volume, the sound speed measures, in m/s, from pixel values in each tomogram, were averaged together to generate the sound speed measurement used as a proxy of breast density.

One experienced rater, who processed UST scans and recorded sound speed measures in the Ultrasound Study of Tamoxifen, trained five raters to process the UST scans. All raters, masked to subject data, performed preanalytic processing of images and recorded the measured sound speed. The baseline and repeat scans were assessed by raters sequentially for each subject to enable determination of common volumes for each pair of scans. Next, four of these raters, including the experienced rater, repeated these measurements on the same scans. For the second review, the scans were randomly reordered, but baseline and follow-up scans for each subject were still read sequentially since this was necessary to identify the common volume.

2.C. Statistical analysis

The inter- and intrarater reliabilities of sound speed measures were assessed using a random effects model containing covariates with potential sources of variation nested within one another (i.e., subject, baseline or follow-

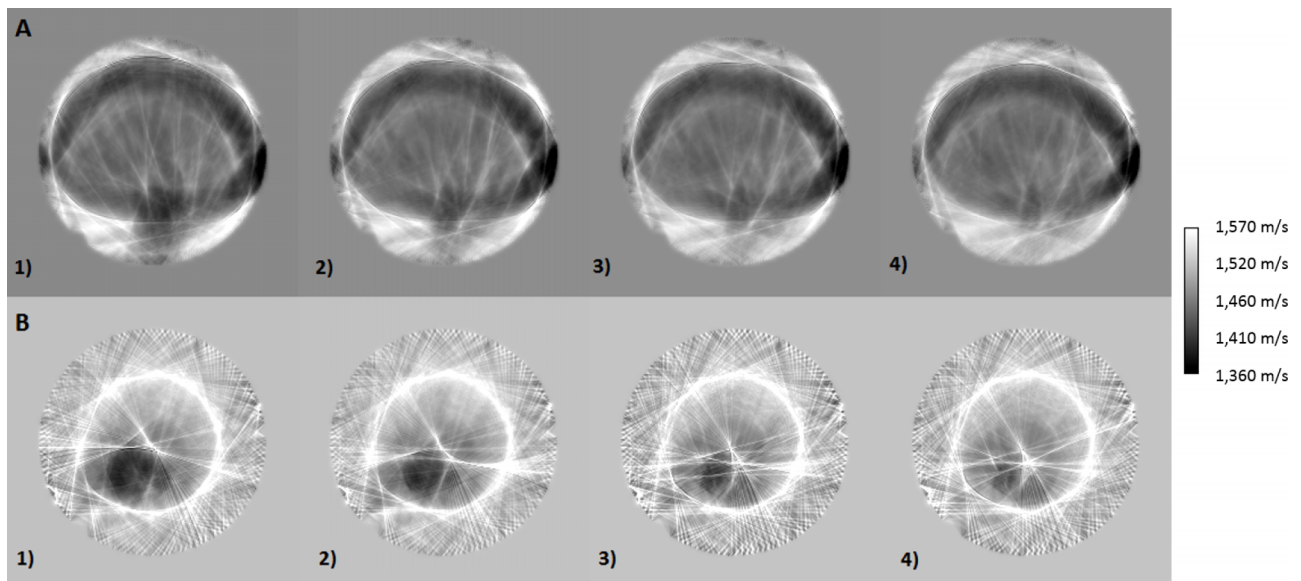


FIG. 2. (A) Selection of starting breast tissue image slice from the first four tomograms, which borders the chest wall. In this example, slice three was chosen to be the first slice without any chest wall present. Slices three and four were included in the final sound speed image stack. (B) Selection of the last breast tissue image slice, which borders the nipple. In this example, slice three was chosen to be the last slice with the nipple present. Slices one, two, and three were therefore included in the final image stack.

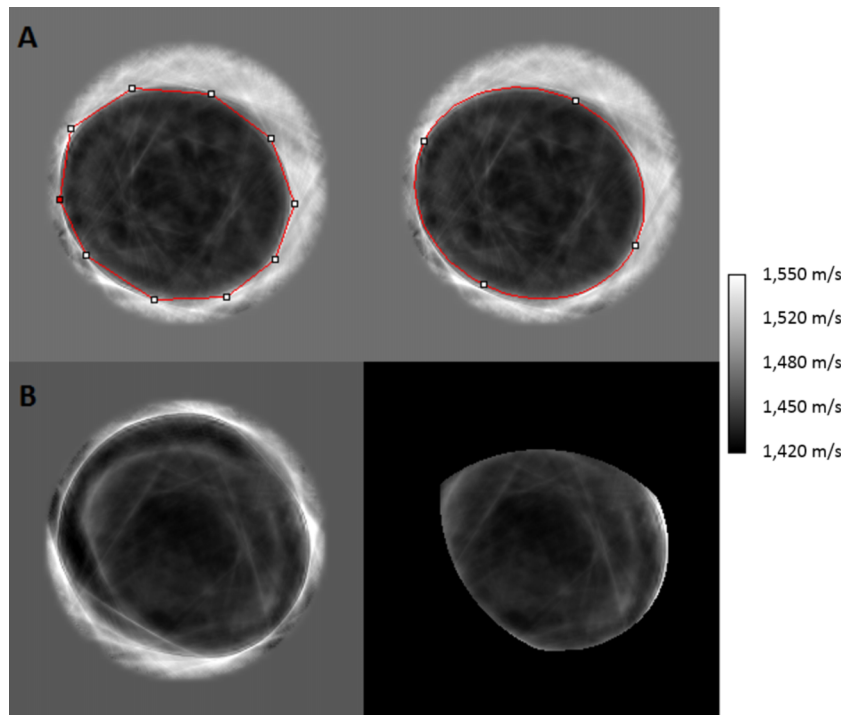


FIG. 3. (A) Depiction of the segmentation algorithm that was utilized to remove sections of each image associated with the water bath: (left) in this example using a midsection slice (free of the artifacts shown in Fig. 2), the breast/water bath interface was first manually selected using 10 points, and second (right), an ellipse was fit to the chosen points to approximate the shape of the breast in the current slice. (B) Sample sound speed image before (left) and after (right) the removal of a dark ring artifact. The images show a portion of a breast dominated by fatty tissues as indicated by dark regions inside the contour (indicating low sound speeds) while the water outside the breast has a higher sound speed and appears whiter.

up scan, rater, and repeat measurements by four of the raters; Fig. 4). An unbalanced model provided the ability to increase statistical power and fully utilize data from all raters, since only four out of the six raters had repeated reads. The percent variation in sound speed attributed to each of these covariates was calculated. Additionally, to assess the reliability of estimating changes in breast density over time, the change in sound speed between the baseline and follow-up scan was assessed. A similar random effects model was used to calculate percent variation in change in sound speed attributed to each covariate. Intraclass correlation coefficients (ICCs) for sound speed and change in sound speed were also calculated based on the experienced rater’s first and second reads. ICC values for strength of agreement were interpreted as slight (0.00–0.20), fair (0.21–0.40), moderate (0.41–0.60), substantial (0.61–0.80), or excellent

(0.81–1.00).²⁹ All analyses were conducted in SAS v9.3 using PROC GLM (2011, SAS Institute, Cary, NC).

3. RESULTS

Among participants included in this analysis ($n = 22$), the median time between baseline and follow-up scans was five months (161 days), ranging from one to 13 months (39–405 days). For both baseline and follow-up scans, the median sound speed measure was 1450 m/s (range: 1430–1480 m/s) and the median change in sound speed between scans was -4.41 m/s (range: -9.48 to 13.04 m/s; Table I). Baseline and follow-up UST sound speeds for each participant are also shown in Fig. 5.

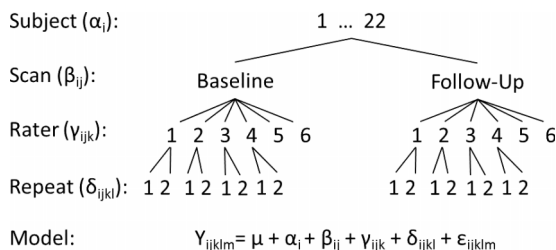


FIG. 4. Unbalanced, nested, random effects model used to calculate percent variation in sound speed attributed to each covariate.

TABLE I. Descriptive statistics for baseline and follow-up scans from UST ($N = 22$).

Measures	Median (range)
UST sound speed measures ^a	
Baseline (m/s)	1450 (1430–1480)
Follow-up (m/s)	1450 (1430–1480)
Change in baseline and follow-up (m/s)	-4.41 (-9.48 to 13.04)
Time between baseline and follow-up	
Months	5 (1–13)
Days	161 (39–405)

Note: N , frequency; UST, ultrasound tomography. ^aFirst reads from the experienced rater.

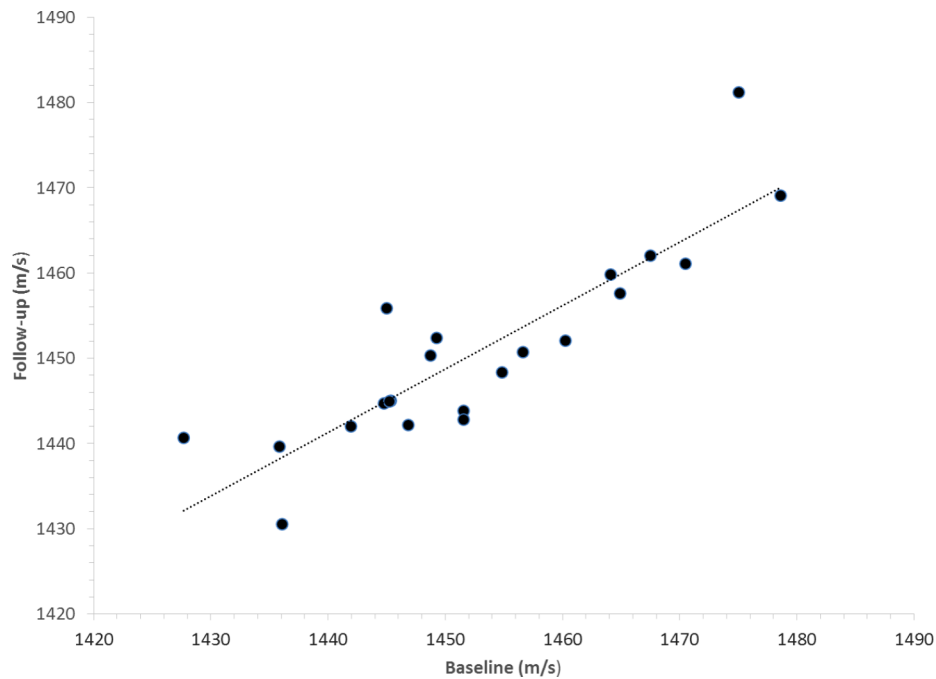


Fig. 5. Scatterplot of baseline and follow-up sound speed measures for each participant as measured by the experienced rater ($N = 22$).

Variation among participants accounted for 86% of the variation in sound speed, with additional contributors including variation between baseline and follow-up scans within subject (7.5%), and differences between the six raters [1.1%, Table II(A)]. The variation for intrarater measurements approached 0%. Results were similar when evaluating change in sound speed between baseline and follow-up scans, with most variation in sound speed due to variability between subjects (62.6%). Variation in change in sound speed estimates attributable to differences between the raters was 2.7% and within raters nearly 0%. For our experienced rater's repeat reads, we observed an excellent level of reproducibility (Fig. 6), with an ICC of 93.3%, for sound speed measures and a substantial level of reproducibility, with an ICC of 70.4%, for change in sound speed [Table II(B)].

4. DISCUSSION

Our results demonstrate that estimates of volumetric breast density, based on UST sound speed measurements, yield excellent inter- and intrarater reliabilities. Most importantly, variations in sound speed measurements were largely a reflection of differences between subjects and, to a lesser

degree, changes between baseline and follow-up scans, with rater being the least likely to contribute to sound speed variations. Additionally, repeat measures performed by the experienced rater showed a high degree of reproducibility for sound speed measures and substantial reproducibility for assessment of change in sound speed between baseline and follow-up UST scans. Given that average sound speed changes within individuals were approximately 4 m/s, these data underscore the sensitivity of UST measurements. These results suggest that UST is a reliable tool for estimating breast density and sensitively detecting changes in its value within individuals over time.

Currently, clinical radiologists routinely report breast density from mammography using visual assessment according to the American College of Radiology's BI-RADS breast density classification as almost entirely fat, scattered fibroglandular densities, heterogeneously dense, and extremely dense.⁴ BI-RADS density assessment has been shown to have substantial intrarater agreement (Cohen's kappa (κ) ranging from 0.64 to 0.90) and moderate inter-rater agreement (κ ranging from 0.44 to 0.77).³⁰⁻³⁵ Most disagreements reflect imprecise separation of the two intermediate density categories, scattered fibroglandular and heterogeneously dense, which are the predominant categories in the general population,

TABLE II. (A) Percent variation in sound speed and change in sound speed attributable to covariates and (B) ICC for the experienced rater's repeat reads for sound speed and change in sound speed.

Measure	(A) Percent variation (%)				(B) ICC (%)
	Subject	Scan	Rater	Repeat	Experienced rater
Sound speed	86.0	7.5	1.1	0	93.3
Change in sound speed	62.6	—	2.7	0	70.4

Note: ICC, intraclass correlation coefficient.

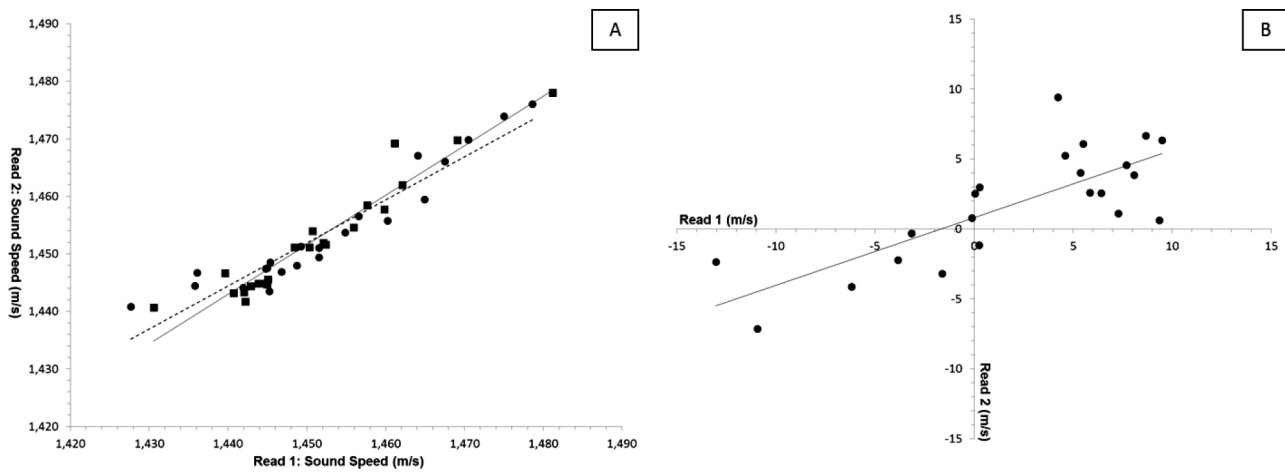


FIG. 6. Scatterplots comparing (A) the repeat reads from the experienced rater's measurements of breast density in sound speed at baseline (round symbols and dotted line) and follow-up (square symbols and solid line) and (B) the change in sound speed between the baseline and follow-up UST scan.

independent of age and menopausal status.^{30,36,37} Accordingly, substantial changes in density may nonetheless represent within category changes, rendering them unapparent with BI-RADS assessment.

Other methods used to visually estimate percent density, using six categories of percent density, have previously shown moderate to high inter- (ICCs ranging from 0.68 to 0.89) and intrarater reliabilities (ICCs ranging from 0.73 to 0.96),^{38–41} and high inter- (ICC = 0.94) and intrarater reliabilities (ICC = 0.96) using 21 categories.⁴² Consistent with the intrarater reliability estimates we observed for sound speed measures, mammographic breast density assessment using quantitative computer-assisted interactive thresholding methods has also yielded high intrarater reliability (correlation coefficients ranging from 0.82 to 0.94).^{39,41,43,44} Thus, the reproducibility of UST density measures compares favorably with other reliable methods for single determinations, especially since UST relies upon quantitative volumetric assessment of sound speed. For estimating changes in density, UST offers the possibility of improved reliability, because of the greater ability to align 3D images, the invariability of sound speed, and the constancy of machine settings, which offers the potential for achieving limited variability in sound speed measurement between scanners.

Growing evidence suggests that a reduction in breast density, among women receiving tamoxifen in either adjuvant treatment or chemoprevention, is predictive of clinical response.^{22–26} The Ultrasound Study of Tamoxifen will assess whether repeated UST sound speed measurements among tamoxifen users can identify declines in density within months. The possibility of distinguishing tamoxifen responders from nonresponders quickly could provide encouragement for adherence among responders and suggest exploration of other options among nonresponders. The value of measuring change in density as a means of screening and risk assessment to predict risk of second contralateral breast cancers,⁴⁵ and to monitor patients receiving combined estrogen plus progestin hormone replacement,⁴⁶ has been studied, but data are limited and not yet conclusive.

Strengths of this analysis include access to the Ultrasound Study of Tamoxifen population, which provided the ability to assess inter- and intrarater reliabilities of UST sound speed measures and, more importantly, serial measures within subjects, affording the opportunity to assess the reliability of change in sound speed. Additionally, we used a method of randomization (i.e., subject scans were randomized, but each subject's baseline and follow-up scans were read sequentially) similar to a past analysis that found this to be a sensitive method for assessing change in breast density as measured from mammography,⁴⁷ although we did not randomize order within subject scans. Another important aspect in the feasibility of future implementation of this technology was the ease in training raters to conduct these measurements. Although results of this analysis are promising, the sample size was limited and future analyses assessing this novel surrogate of breast density are needed. To maximize statistical power, we used multiple raters to assess between ($n = 6$) and within rater ($n = 4$) reliability and analyzed all data in one efficient model. Future goals include reducing the amount of manual modifications needed to remove dark ring artifacts. Finally, whereas we assessed determinants of the reliability of sound speed estimates averaged across the total breast volume, prior studies have suggested that localized breast density measures may prove to be informative with respect to risk prediction.^{48,49} Work to determine whether sound speed changes are uniform throughout the breast or show regional variation is ongoing in this study population. It is conceivable that UST imaging may permit better assessment of this process than mammography because of the possibility of 3D alignment of serial images, but the reliability of localized sound speed estimates will require future evaluation.

Serial measurement of breast density may represent a potential approach for enhancing risk assessment beyond what is achievable with single measurements. This early study suggests that UST represents a promising method for serially assessing breast density with high precision, 3D assessment without compression of the breast, and avoidance of radiation. Currently, research studies focused on determining factors

that contribute to change in breast density are limited by the existing methods of measurement. UST may represent a technique for advancing this area of research.

ACKNOWLEDGMENTS

This research was supported in part by the Intramural Research Program of the National Institutes of Health, National Cancer Institute. The authors are indebted to the participants in the Ultrasound Study of Tamoxifen for dedicating their valuable time and to the physicians, nurses, technologists, and interviewers for their efforts in the field. The authors thank Vivian Linke and Tiffany Drane for research assistance. The authors also thank Beth Slotman and Kerry Grace Morrissey from Westat for study management support. N. Duric and P. Littrup are coinventors of and have intellectual property interests in the ultrasound technology used for the measurements described in this paper. The remaining authors declare that they have no conflicts of interest.

^{a)}Author to whom correspondence should be addressed. Electronic mail: GierachG@mail.nih.gov; Telephone: (240) 276-7299; Fax: (240) 276-7838.

¹V. A. McCormack and I. d. S. Silva, "Breast density and parenchymal patterns as markers of breast cancer risk: A meta-analysis," *Cancer Epidemiol., Biomarkers Prev.* **15**, 1159–1169 (2006).

²J. N. Wolfe, "Risk for breast cancer development determined by mammographic parenchymal pattern," *Cancer* **37**, 2486–2492 (1976).

³N. F. Boyd, L. J. Martin, M. Bronskill, M. J. Yaffe, N. Duric, and S. Minkin, "Breast tissue composition and susceptibility to breast cancer," *J. Natl. Cancer Inst.* **102**, 1224–1237 (2010).

⁴C. D'orsi et al., "BI-RADS: Mammography," in *Breast Imaging Reporting and Data System: ACR BI-RADS – Breast Imaging Atlas*, edited by C. D'orsi et al. (American College of Radiology, Reston, VA, 2003).

⁵M. J. Yaffe, "Mammographic density. Measurement of mammographic density," *Breast Cancer Res.* **10**, 209 (2008).

⁶S. Ciatto, D. Bernardi, M. Calabrese, M. Durando, M. A. Gentilini, G. Mariscotti, F. Monetti, E. Moriconi, B. Pesce, A. Roselli, C. Stevanin, M. Tapparelli, and N. Houssami, "A first evaluation of breast radiological density assessment by QUANTRA software as compared to visual classification," *Breast* **21**, 503–506 (2012).

⁷J. Wang, A. Azziz, B. Fan, S. Malkov, C. Klifa, D. Newitt, S. Yitta, N. Hylton, K. Kerlikowske, and J. A. Shepherd, "Agreement of mammographic measures of volumetric breast density to MRI," *PLoS One* **8**, e81653 (2013).

⁸D. B. Kopans, "Basic physics and doubts about relationship between mammographically determined tissue density and breast cancer risk," *Radiology* **246**, 348–353 (2008).

⁹J. E. Olson, T. A. Sellers, C. G. Scott, B. A. Schueler, K. R. Brandt, D. J. Serie, M. R. Jensen, F. F. Wu, M. J. Morton, J. J. Heine, F. J. Couch, V. S. Pankratz, and C. M. Vachon, "The influence of mammogram acquisition on the mammographic density and breast cancer association in the Mayo Mammography Health Study cohort," *Breast Cancer Res.* **14**, R147 (2012).

¹⁰A. B. de Gonzalez, C. D. Berg, K. Visvanathan, and M. Robson, "Estimated risk of radiation-induced breast cancer from mammographic screening for young BRCA mutation carriers," *J. Natl. Cancer Inst.* **101**, 205–209 (2009).

¹¹S. J. Graham, M. J. Bronskill, J. W. Byng, M. J. Yaffe, and N. F. Boyd, "Quantitative correlation of breast tissue parameters using magnetic resonance and x-ray mammography," *Br. J. Cancer* **73**, 162–168 (1996).

¹²M. C. Pike and C. L. Pearce, "Mammographic density, MRI background parenchymal enhancement and breast cancer risk," *Ann. Oncol.* **24**(Suppl. 8), viii37–viii41 (2013).

¹³D. J. Thompson, M. O. Leach, G. Kwan-Lim, S. A. Gayther, S. J. Ramus, I. Warsi, F. Lennard, M. Khazen, E. Bryant, S. Reed, C. R. Boggis, D. G. Evans, R. A. Eeles, D. F. Easton, and R. M. Warren, "Assessing the

usefulness of a novel MRI-based breast density estimation algorithm in a cohort of women at high genetic risk of breast cancer: The UK MARIBS study," *Breast Cancer Res.* **11**, R80 (2009).

¹⁴N. Duric, P. Littrup, L. Poulou, A. Babkin, R. Pevzner, E. Holsapple, O. Rama, and C. Glide, "Detection of breast cancer with ultrasound tomography: First results with the computed ultrasound risk evaluation (CURE) prototype," *Med. Phys.* **34**, 773–785 (2007).

¹⁵C. Glide, N. Duric, and P. Littrup, "Novel approach to evaluating breast density utilizing ultrasound tomography," *Med. Phys.* **34**, 744–753 (2007).

¹⁶N. Duric, P. Littrup, S. Schmidt, C. Li, O. Roy, L. Bey-Knight, R. Janer, D. Kunz, X. Chen, J. Goll, A. Wallen, F. Zafar, V. Allada, E. West, I. Jovanovic, K. Li, and W. Greenway, "Breast imaging with the SoftVue imaging system: First results," *Proc. SPIE* **8675**, 86750K (2013).

¹⁷N. Duric, N. Boyd, P. Littrup, M. Sak, L. Myc, C. Li, E. West, S. Minkin, L. Martin, M. Yaffe, S. Schmidt, M. Faiz, J. Shen, O. Melnichouk, Q. Li, and T. Albrecht, "Breast density measurements with ultrasound tomography: A comparison with film and digital mammography," *Med. Phys.* **40**, 013501 (12pp.) (2013).

¹⁸M. Sak, N. Duric, P. Littrup, C. Li, L. Bey-Knight, M. Sherman, N. Boyd, and G. Gierach, "Breast density measurements using ultrasound tomography for patients undergoing tamoxifen treatment," *Proc. SPIE* **8675**, 86751E (2013).

¹⁹M. Sak, N. Duric, N. Boyd, P. Littrup, L. Myc, M. Faiz, C. Li, and L. Bey-Knight, "Relationship between breast sound speed and mammographic percent density," *Proc. SPIE* **7968**, 79680N (2011).

²⁰W. Weiwad, A. Heinig, L. Goetz, H. Hartmann, D. Lampe, J. Buchmann, R. Millner, R. P. Spielmann, and S. H. Heywang-Koebrunner, "Direct measurement of sound velocity in various specimens of breast tissue," *Invest. Radiol.* **35**, 721–726 (2000).

²¹C. K. Glide-Hurst, N. Duric, and P. Littrup, "Volumetric breast density evaluation from ultrasound tomography images," *Med. Phys.* **35**, 3988–3997 (2008).

²²J. Cuzick, J. Warwick, E. Pinney, S. W. Duffy, S. Cawthorn, A. Howell, J. F. Forbes, and R. M. Warren, "Tamoxifen-induced reduction in mammographic density and breast cancer risk reduction: A nested case-control study," *J. Natl. Cancer Inst.* **103**, 744–752 (2011).

²³J. Kim, W. Han, H. G. Moon, S. K. Ahn, H. C. Shin, J. M. You, S. W. Han, S. A. Im, T. Y. Kim, H. R. Koo, J. M. Chang, N. Cho, W. K. Moon, and D. Y. Noh, "Breast density change as a predictive surrogate for response to adjuvant endocrine therapy in hormone receptor positive breast cancer," *Breast Cancer Res.* **14**, R102 (2012).

²⁴J. Li, K. Humphreys, L. Eriksson, G. Edgren, K. Czene, and P. Hall, "Mammographic density reduction is a prognostic marker of response to adjuvant tamoxifen therapy in postmenopausal patients with breast cancer," *J. Clin. Oncol.* **31**, 2249–2256 (2013).

²⁵K. L. Ko, I. S. Shin, J. Y. You, S. Y. Jung, J. Ro, and E. S. Lee, "Adjuvant tamoxifen-induced mammographic breast density reduction as a predictor for recurrence in estrogen receptor-positive premenopausal breast cancer patients," *Breast Cancer Res. Treat.* **142**, 559–567 (2013).

²⁶S. J. Nyante, M. E. Sherman, R. M. Pfeiffer, A. Berrington de Gonzalez, L. A. Brinton, E. J. Aiello Bowles, R. N. Hoover, A. Glass, and G. L. Gierach, "Prognostic significance of mammographic density change after initiation of tamoxifen for ER-positive breast cancer," *J. Natl. Cancer Inst.* **107**, dju425 (2015).

²⁷N. Duric, P. Littrup, A. Babkin, D. Chambers, S. Azevedo, R. Pevzner, M. Tokarev, E. Holsapple, O. Rama, and R. Duncan, "Development of ultrasound tomography for breast imaging: Technical assessment," *Med. Phys.* **32**, 1375–1386 (2005).

²⁸C. A. Schneider, W. S. Rasband, and K. W. Eliceiri, "NIH image to ImageJ: 25 years of image analysis," *Nat. Methods* **9**, 671–675 (2012).

²⁹J. R. Landis and G. G. Koch, "The measurement of observer agreement for categorical data," *Biometrics* **33**, 159–174 (1977).

³⁰K. Kerlikowske, D. Grady, J. Barclay, S. D. Frankel, S. H. Ominsky, E. A. Sickles, and V. Ernster, "Variability and accuracy in mammographic interpretation using the American College of Radiology breast imaging reporting and data system," *J. Natl. Cancer Inst.* **90**, 1801–1809 (1998).

³¹S. Ciatto, N. Houssami, A. Apruzzese, E. Bassetti, B. Brancato, F. Carozzi, S. Catarzi, M. P. Lamberini, G. Marcelli, R. Pellizzoni, B. Pesce, G. Rizzo, F. Russo, and A. Scorsolini, "Categorizing breast mammographic density: Intra- and interobserver reproducibility of BI-RADS density categories," *Breast* **14**, 269–275 (2005).

³²A. Redondo, M. Comas, F. Macia, F. Ferrer, C. Murta-Nascimento, M. T. Maristany, E. Molins, M. Sala, and X. Castells, "Inter- and intraradiologist

- variability in the BI-RADS assessment and breast density categories for screening mammograms," *Br. J. Radiol.* **85**, 1465–1470 (2012).
- ³³W. A. Berg, C. Campassi, P. Langenberg, and M. J. Sexton, "Breast imaging reporting and data system: Inter- and intraobserver variability in feature analysis and final assessment," *Am. J. Roentgenol.* **174**, 1769–1777 (2000).
- ³⁴E. A. Ooms, H. M. Zonderland, M. J. Eijkemans, M. Kriege, B. M. Delavary, C. W. Burger, and A. C. Ansink, "Mammography: Interobserver variability in breast density assessment," *Breast* **16**, 568–576 (2007).
- ³⁵M. Garrido-Esteva, F. Ruiz-Perales, J. Miranda, N. Asuncion, I. Gonzalez-Roman, C. Sanchez-Contador, C. Santamarina, P. Moreo, C. Vidal, M. Peris, M. P. Moreno, J. A. Vaquez-Carrete, F. Collado-Garcia, F. Casanova, M. Ederra, D. Salas, and M. Pollan, "Evaluation of mammographic density patterns: Reproducibility and concordance among scales," *BMC Cancer* **10**, 485 (2010).
- ³⁶K. Kerlikowske, L. Ichikawa, D. L. Miglioretti, D. S. Buist, P. M. Vacek, R. Smith-Bindman, B. Yankaskas, P. A. Carney, and R. Ballard-Barbash, "Longitudinal measurement of clinical mammographic breast density to improve estimation of breast cancer risk," *J. Natl. Cancer Inst.* **99**, 386–395 (2007).
- ³⁷B. L. Sprague, R. E. Gangnon, V. Burt, A. Trentham-Dietz, J. M. Hampton, R. D. Wellman, K. Kerlikowske, and D. L. Miglioretti, "Prevalence of mammographically dense breasts in the United States," *J. Natl. Cancer Inst.* **106**, dju255 (2014).
- ³⁸R. Jong, E. Fishell, L. Little, G. Lockwood, and N. F. Boyd, "Mammographic signs of potential relevance to breast cancer risk: The agreement of radiologists' classification," *Eur. J. Cancer Prev.* **5**, 281–286 (1996).
- ³⁹N. F. Boyd, J. W. Byng, R. A. Jong, E. K. Fishell, L. E. Little, A. B. Miller, G. A. Lockwood, D. L. Tritchler, and M. J. Yaffe, "Quantitative classification of mammographic densities and breast cancer risk: Results from the Canadian national breast screening study," *J. Natl. Cancer Inst.* **87**, 670–675 (1995).
- ⁴⁰J. Benichou, C. Byrne, L. A. Capece, L. E. Carroll, K. Hurt-Mullen, D. Y. Pee, M. Salane, C. Schairer, and M. H. Gail, "Secular stability and reliability of measurements of the percentage of dense tissue on mammograms," *Cancer Detect. Prev.* **27**, 266–274 (2003).
- ⁴¹N. F. Boyd, H. Guo, L. J. Martin, L. Sun, J. Stone, E. Fishell, R. A. Jong, G. Hislop, A. Chiarelli, S. Minkin, and M. J. Yaffe, "Mammographic density and the risk and detection of breast cancer," *N. Engl. J. Med.* **356**, 227–236 (2007).
- ⁴²J. Gao, R. Warren, H. Warren-Forward, and J. F. Forbes, "Reproducibility of visual assessment on mammographic density," *Breast Cancer Res. Treat.* **108**, 121–127 (2008).
- ⁴³C. Byrne, S. E. Hankinson, M. Pollak, W. C. Willett, G. A. Colditz, and F. E. Speizer, "Insulin-like growth factors and mammographic density," *Growth Horm. IGF Res.* **10**(Suppl. A), S24–S25 (2000).
- ⁴⁴C. G. Woolcott, S. M. Conroy, C. Nagata, G. Ursin, C. M. Vachon, M. J. Yaffe, I. S. Pagano, C. Byrne, and G. Maskarinec, "Methods for assessing and representing mammographic density: An analysis of 4 case-control studies," *Am. J. Epidemiol.* **179**, 236–244 (2013).
- ⁴⁵M. E. Sandberg, J. Li, P. Hall, M. Hartman, I. dos-Santos-Silva, K. Humphreys, and K. Czene, "Change of mammographic density predicts the risk of contralateral breast cancer—a case-control study," *Breast Cancer Res.* **15**, R57 (2013).
- ⁴⁶N. F. Boyd, O. Melnichouk, L. J. Martin, G. Hislop, A. M. Chiarelli, M. J. Yaffe, and S. Minkin, "Mammographic density, response to hormones, and breast cancer risk," *J. Clin. Oncol.* **29**, 2985–2992 (2011).
- ⁴⁷J. Stone, A. Gunasekara, L. J. Martin, M. Yaffe, S. Minkin, and N. F. Boyd, "The detection of change in mammographic density," *Cancer Epidemiol., Biomarkers Prev.* **12**, 625–630 (2003).
- ⁴⁸G. Ursin, L. Hovanesian-Larsen, Y. R. Parisky, M. C. Pike, and A. H. Wu, "Greatly increased occurrence of breast cancers in areas of mammographically dense tissue," *Breast Cancer Res.* **7**, R605–R608 (2005).
- ⁴⁹S. M. P. Pereira, V. A. McCormack, J. H. Hipwell, C. Record, L. S. Wilkinson, S. M. Moss, D. J. Hawkes, and I. dos-Santos-Silva, "Localized fibroglandular tissue as a predictor of future tumor location within the breast," *Cancer Epidemiol., Biomarkers Prev.* **20**, 1718–1725 (2011).